07,11,12,13

Rotator Phases during Heating of Odd Normal Alkanes: Heneicosane, Tricosane, and Pentacosane

© A.K. Borisov, S.A. Gureva, V.A. Marikhin

Ioffe Institute,
St. Petersburg, Russia

E-mail: borisov.ak@mail.ioffe.ru

Received August 26, 2025
Revised August 27, 2025
Accepted August 27, 2025

Phase transitions during heating in odd normal alkanes, characterized by orthorhombic unit cell symmetry at room temperature, were investigated by differential scanning calorimetry. The analysis of thermograms revealed the presence of a series of crystalline and rotator phases during the transition from the solid to the liquid state. The phase transformations were characterized from the perspective of heterogeneous process development based on the theory of diffuse phase transitions. A similar multi-stage mechanism of phase transitions was established for the three normal alkane homologs. For the first time, it was found that the transition from the initial crystalline phase to the rotator phase occurs in a uniform manner in heneicosane (C21), tricosane (C23), and pentacosane (C25) via two intermediate crystalline phases: $O_i \rightarrow O_{dci} \rightarrow M_{dci} \rightarrow R_V$. The subsequent transition to the liquid state in heneicosane proceeds through two rotator phases: $R_V \Rightarrow R_I \rightarrow$ liquid liquid, whereas in tricosane and pentacosane the phase sequence was found to be more complex: $R_V \Rightarrow R_I \rightarrow R_{II} \rightarrow$ liquid liquid.

Keywords: phase transitions, rotator phases, n-alkanes, molecular crystals, calorimetry.

DOI: 10.61011/PSS.2025.09.62358.237-25

1. Introduction

One of the priority fields of development of modern science is to search for ways of going over to environmentally friendly („green“) and resource-saving energy. One of the possible methods of solving this problem is development of phase change materials (PCM) with improved operating properties. The PCMs can absorb, store and release flows of thermal energy in an unlimited number of times from various external sources due to intrinsic thermal effects. In order to provide operation within a pre-defined temperature range, an optimal PCM is selected, determining a suitable temperature of the phase transition that provides accumulation or release of heat within this interval.

As the PCM, long-chain molecular crystals (LCMC) can provide conditions of comfortable human activity and operation of equipment in conditions of both decreased and increase temperatures from -50 to $+80\,^{\circ}$C. The LCMCs have a unique property — it is possible to select the operating temperature range by varying a length of the molecule chain, i.e. selecting a required homolog, which, combined with high capacity, makes them ones of the most promising PCMs.

Wide PCM distribution requires improvement of practically important characteristics of the materials. But basics of phase transformations in substances from which these materials are manufactured are still understudied. The present study is aimed at solving this problem in relation to the LCMCs of normal alkanes.

The normal alkanes (n-alkanes) of a chemical formula C_nH_{2n+2} are the most simple in terms of an LCMC structure. Moreover, it is possible to produce monodisperse samples of a high purity degree, thereby making them the most preferable for fundamental thermodynamic research.

At the room temperature, odd n-alkanes with a chain length from 9 to 45 carbon atoms have an orthorhombic symmetry of basic cells and subcells [1,2]. A symmetry type of molecule packing in the even and odd n-alkanes is induced by specific features of symmetry of their (trans- or cis-) molecules that affect arrangement of end methyl groups.

It is found that with an increase of the temperature the n-alkanes transit into rotation phases that are an intermediate state between a crystal and a liquid, which is characterized by origination of molecular rotation around their main axes [3,4].

There are five distinguished rotator phases (R_I–R_V) that are different by a symmetry type and a number of possible orientations of the molecules [5,6]. Three of them are well characterized: R_I, R_{II} and R_V that are manifested exactly in the n-alkanes when $n < 27$ carbon atoms [7–12]. In the structure R_I, the molecules are packed vertically with orthorhombic symmetry at a two-layer sequence of ABAB packing of lamellae. The phase R_{II} is also characterized by vertically arranged molecules in the lamellae, but with a three-layer ABC packing and true hexagonal (rhombohedral) symmetry of the molecule packing. The molecules in the phase R_V are packed with monoclinic symmetry in the lamellae that in turn have the ABAB packing. The other phases, R_{III} and R_{IV}, are noticeably more poorly studied are typical for longer n-alkanes and we do not consider them therefore.

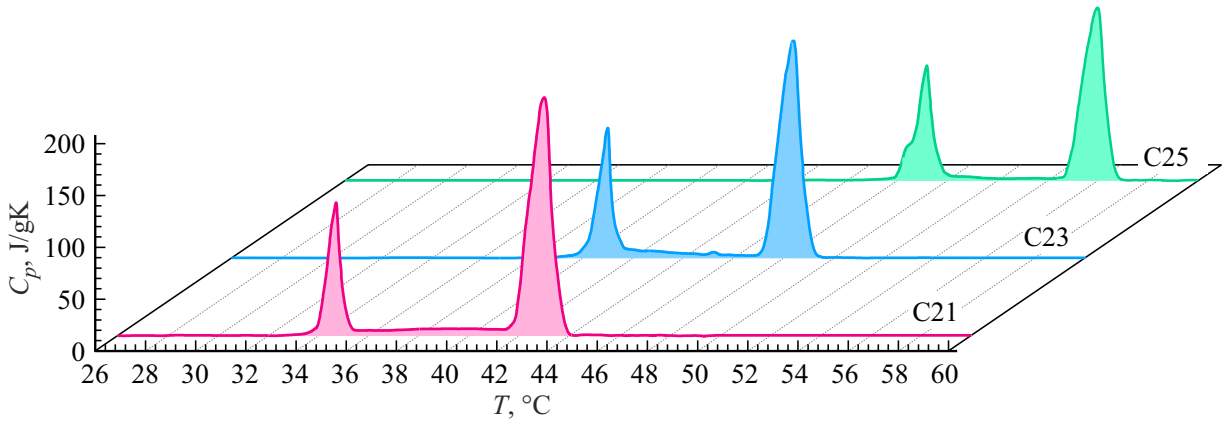

Figure 1. DSC heating thermograms within a range of phase transition of the n-alkanes: $C_{21}H_{44}$ (pink), $C_{23}H_{48}$ (blue), $C_{25}H_{52}$ (green).

2. Experiment

In order to find a mechanism of structure transformations, the following odd n-alkanes were studied by differential scanning calorimetry (DSC): heneicosane $C_{21}H_{44}$ (C21), tricosane $C_{23}H_{48}$ (C23) and pentacosane $C_{25}H_{52}$ (C25).

Samples to be studied were monodisperse n-alkanes produced by Sigma-Aldrich with purity of $> 99.0\,\%$. Thermal properties were determined in a calorimeter Henven HSC-4 (China) in the nitrogen atmosphere. A weight of tested samples was selected to be ~ 10 mg, which is enough for recording low-energy transitions between the rotator phases, but at the same time providing minimization of thermal resistance of a calorimetry cell. A scanning rate was selected to be $0.5\,^{\circ}$C/min, which was optimal for the samples of the given mass, on the one hand, to achieve the best resolution of peaks of heat capacity and, on the other hand, to ensure heat capacity that was enough for recording intensity. The measurements were performed within the temperature range from 10 to $70\,^{\circ}$C.

Figure 1 shows the DSC thermograms of the studied n-alkanes within the range of phase transitions, which are obtained during heating at the rate of $0.5\,^{\circ}$C/min. It was previously found [2,13,14] that the n-alkanes are characterized by two types of the phase transitions manifested as peaks on the DSC curves. The low-temperature endothermic peak during heating is related to a structure transition inside a solid phase, while the high-temperature peak is related to a transition from the ordered structure to disorder (melting). It can be noted from analysis of Figure 1 that the studied n-alkanes demonstrate presence of two pronounced peaks in the transition between the crystal and the liquid. However, more detailed analysis also shows presence of weak endothermic effects that are predominantly manifested between the base peaks. It can be assumed that these effects can be related to the transitions between the rotator phases.

3. Results and discussion

Among the three homologs in question, presently, the most fully studied in the literature are the phase transformations exactly for C23, in particular, we have in detail studied kinetics of polymorphous transformations by a combination of synchronous X-ray diffractometry and DSC [15]. Based on the literature data [5–8,12,16–18] and our own results, we have found the following sequence of the phase transitions of a different nature in C23:

$$O_i \xrightarrow[38\,^{\circ}\mathrm{C}]{} O_{dci} \xrightarrow[40-41\,^{\circ}\mathrm{C}]{} R_V \underset{41-42\,^{\circ}\mathrm{C}}{\Longrightarrow}$$

$$R_I \xrightarrow[45\,^{\circ}\mathrm{C}]{} R_{II} \xrightarrow[47-48\,^{\circ}\mathrm{C}]{} \text{liquid},$$

where O_i is a low-temperature orthorhombic crystal phase ($Pbcm$ (57)), O_{dci} is a high-temperature orthorhombic crystal phase ($Pbnm$ (62)), R_V is a monoclinic rotator phase (Aa (9)), R_I is an orthorhombic rotator phase ($Fmmm$ (69)), R_{II} is a rhombohedral (hexagonal) rotator phase ($R\bar{3}m$ (166)), $R_V \underset{41-42\,^{\circ}\mathrm{C}}{\Longrightarrow} R_I$ — a continuous second-order transition.

It can be assumed that the nearest odd homologs with the same initial structure shall exhibit a similar sequence of the solid-solid phase transitions. However, the literature has controversies for origination of the monoclinic rotator phase R_V in the homologs C23 and C25. For example, authors of the study [19] confirm that all the above-said polymorphous modifications appear in C25, but negate appearance of the monoclinic phase in C23. In the studies [17,20], the authors found all the listed polymorphous modifications both in C23 and C25, meanwhile distinguishing for the latter an additional monoclinic phase M_{dci} (Aa) when $T \approx 46-47\,^{\circ}$C, which precedes the rotary one R_V and has the same space group. The authors of the study [18] also distinguish for C25 the monoclinic non-rotator phase, but find a non-rotator phase $Fmmm$ instead of the phase R_V for both the homologs C23 and C25. Based on the above-given literature data as well as data of the

Thermodynamic parameters of the diffuse solid-solid phase transitions in heneicosane (C21), tricosane (C23) and pentacosane (C25)

Sample Peak	No.	T_{max}, °C	C_{max}, J/gK	ΔH, J/g	ω, nm^3
C21	1	33.3	117.7	19.3	672
	2	33.7	38.5	59.2	220
C23	1	40.6	46.0	30.9	328
	2	41.0	106.0	48.4	308
	3	45.2	5.5	7.5	24604
C25	1	47.5	30.0	19.8	547
	2	48.1	107.5	65.7	178

study [2], one can expect the following phase sequence and transitions between them in C25:

$$O_i \xrightarrow[38\,^\circ\mathrm{C}]{} O_{dci} \xrightarrow[44-46\,^\circ\mathrm{C}]{} M_{dci}/R_V \xrightarrow[46-48\,^\circ\mathrm{C}]{} R_I \xrightarrow[49-50\,^\circ\mathrm{C}]{} R_{II} \xrightarrow[52-53\,^\circ\mathrm{C}]{} \text{liquid}.$$

In spite of similarity of the homolog C21 to C23, the literature does not consider the above-give wide and controversial sequence of the phase transitions for it. It is found for C21 that the initial orthorhombic phase O_i ($Pbcm$ (57)) transits only into the orthorhombic rotator phase R_I ($Fmmm$ (69)) [2,5,6,11]. However, it is also noted in the study [18] that the non-rotator phase $Fmmm$ is originated in C21 as well. Thus, the phase sequence can be as follows:

$$O_i \xrightarrow[32\,^\circ\mathrm{C}]{} Fmmm/R_I \xrightarrow[40\,^\circ\mathrm{C}]{} \text{liquid}.$$

It should be noted that the most intense solid-solid phase transition in the DSC thermograms is attributed by the authors of the study [18] to transitions of an order-disorder type (o−d), since it includes significant changes of orientation of the molecules around their main axis — rotation appears. Thus, this solid-solid phase transition is a transition into a rotator phase and can not be attributed to the transition into the non-rotator phase $Fmmm$. However, a non-rotator phase that is similar in the structure and precedes the transition into the rotator state can occur.

The solid-solid phase transitions in the n-alkanes are attributed to diffuse phase transitions (DPT), since their half-width is 1−2 K („diffuse“ in the temperature) [21]. The DPT theory [22–24] presupposes fluctuation formation of nuclei of a new phase with origination of an interphase boundary. The new phase propagates sequentially via layering of the nuclei, where each new stage is accompanied by a slight change of the temperature (ΔT), thereby determining a heterogeneous mechanisms of DPT kinetics.

According to the DPT theory, the peaks of heat capacity shall have a symmetrical Λ-like form. It is shown by experimental data that our peaks PT-1 have asymmetry, thereby making it possible to expand them into symmetrical components using a previously developed method [25]. One of the criteria for this separation is a condition that the enthalpy of the experimentally-obtained peak is equal to a sum of enthalpies of its components. All the studied samples exhibited presence of two symmetrical components and, consequently, we consider development of these solid-solid phase transitions as a two-stage one. The thermograms of the solid-solid phase transitions and their expansions into the symmetrical components are shown in Figure 2.

According to the DPT theory, the symmetrical Λ-like peaks of heat capacity are described by the following relationship:

$$\Delta C_p(T) = 4\Delta C_m \exp\left(B\,\frac{T-T_0}{T_0}\right)\left[1+\exp\left(B\,\frac{T-T_0}{T_0}\right)\right]^{-2}, \quad (1)$$

where T_0 is a temperature of the phase transition; ΔC_m — a maximum value of heat capacity when $T = T_0$; B is an athermal parameter.

Nanonucleus volumes ω are calculated based on a shape of the peaks of heat capacity $C_p(T)$ via the athermal parameter B that characterizes a material structure and affects a degree of phase transition smearing in the temperature. A relation of the parameter B with the nucleus volume ω is determined according to the study [26]:

$$\omega = \frac{BkT}{\rho q_0}, \quad (2)$$

where q_0 is a conversion enthalpy, ρ is a density of the substance, k is the Boltzmann's constant.

The relationships (1) and (2) were used to calculate the elementary volumes ω. Results of the calculations of ω_i as well as the thermodynamic parameters of the solid-solid phase transitions are provided in Table. The peak numbers are marked on Figure 2.

All the samples have a peak of the main solid-solid phase transition expanded into two symmetrical peaks according to the DPT theory (No. 1 and No. 2). For C23, at the higher temperature, we managed to additionally distinguish the diffuse phase transition that also has a symmetrical form of the peak (the peak No. 3).

Based on the obtained thermograms and the analysis performed according to the DPT theory, in accordance with the literature data one can find a sequence of the phase transformations for each of the samples (Figure 2). It is clear from the figure that positions and forms of the endothermic effects on the DSC curves are similar for C21, C23 and C25. It can be concluded that the phase transitions develop similarly in all the three homologs, but there can be some differences due to a length of the molecules.

In C21, at the temperature of 31.4 °C, a deviation from the base line is observed, which can be related to the transition $O_i \rightarrow O_{dci}$ similar to the longer n-alkanes. At 32.8 °C, the DPT with a peak at 33.3 °C starts, which is probably related to origination of the phase M_{dci} (Aa) that almost immediately starts transiting into the rotator phase R_V via the DPT with a peak at 33.7 °C. Then, a

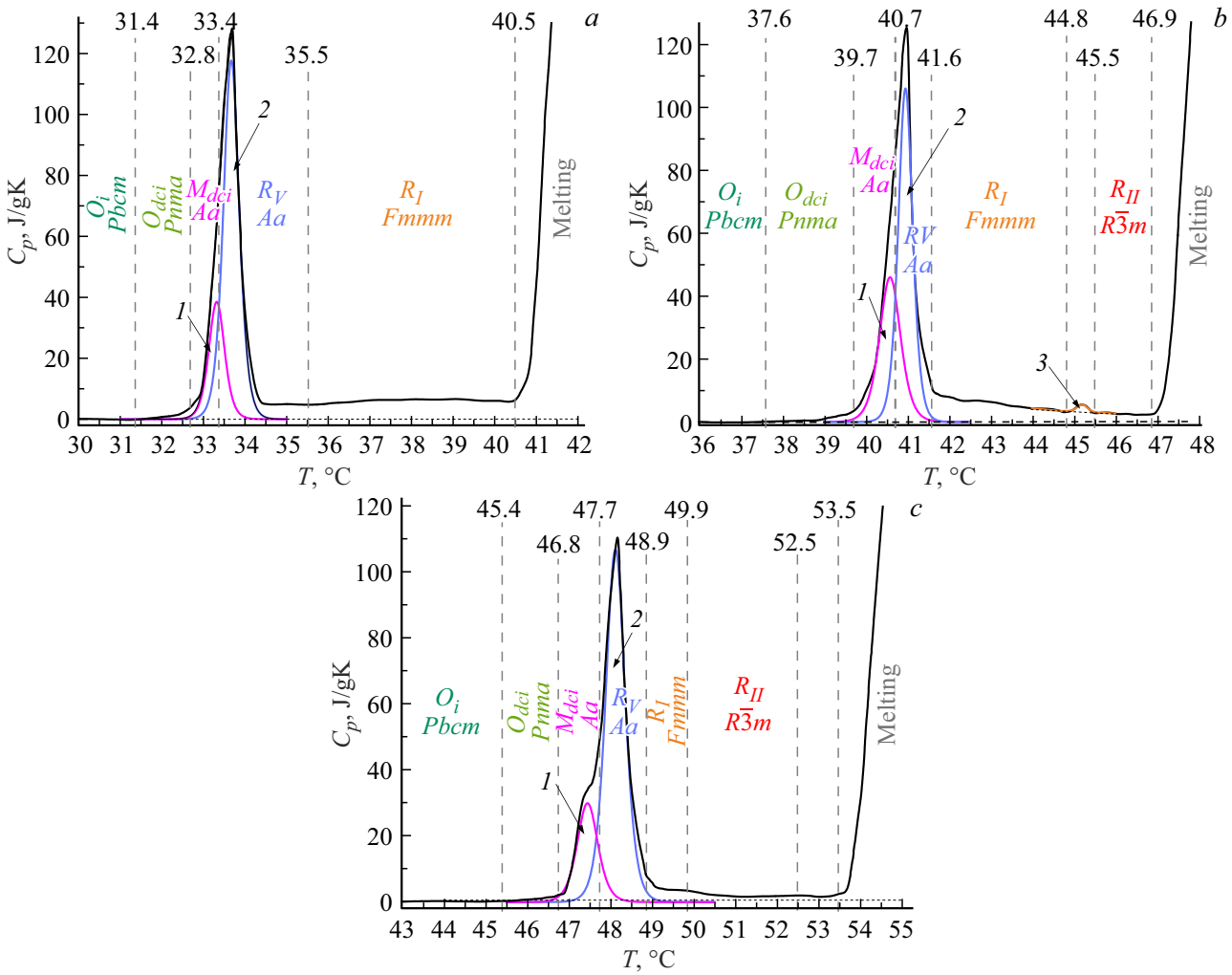

Figure 2. Phase sequence when heating the n-alkanes C21 (*a*), C23 (*b*) and C25 (*c*), which is marked on the DSC thermograms. The digits marks DPTs that are selected among all the solid-solid phase transitions.

deviation from the base line within the temperature range 35.7–40.0 °C is observed and is probably related to the continuous transition into the phase R_I. We used a method of synchrotron X-ray diffractometry to show that a second-order phase transition is observed in C23 and it is related to the transition of the phase R_V into R_I and manifested on the DSC curves as a protracted endothermic effect [15]. At 40.5 °C, the crystal starts melting. Thus, the following phase sequence can be assumed for C21:

$$O_i \xrightarrow[31.4\,^\circ\mathrm{C}]{} O_{dci} \xrightarrow[33.3\,^\circ\mathrm{C}]{} M_{dci} \xrightarrow[33.7\,^\circ\mathrm{C}]{} R_V \underset{35.7-40.4\,^\circ\mathrm{C}}{\Longrightarrow} R_I \xrightarrow[40.5\,^\circ\mathrm{C}]{} \text{liquid}.$$

In C23, the initial sequence of the transitions is similar to C21. The transition $O_i \rightarrow O_{dci}$ at 37.6 °C; the transition $O_{dci} \rightarrow M_{dci}$ at 40.6 °C, the transition $M_{dci} \rightarrow R_V$ at 41.0 °C. Our previous study [15] has not analyzed the DSC thermograms according to the DPT theory, which resulted in neglecting the transition $O_{dci} \rightarrow M_{dci}$. But a noticeable change of the X-ray patterns was observed in this range, which can also confirm presence of an intermediate non-rotator phase M_{dci}. Further in the temperature, the continuous transition $R_V \rightarrow R_I$ follows, which, unlike C21, in C23 starts just after the transition into the phase R_V around 41.6 °C and proceeds up to 44.8 °C. Besides, C23 exhibits a peak at 45.2 °C, which is weak in intensity, but symmetrical in the form and corresponds to the DPT into the phase R_{II}. At 46.9 °C, melting starts. Then, the phase sequence in C23 will be as follows:

$$O_i \xrightarrow[37.6\,^\circ\mathrm{C}]{} O_{dci} \xrightarrow[40.6\,^\circ\mathrm{C}]{} M_{dci} \xrightarrow[41.0\,^\circ\mathrm{C}]{} R_V \underset{41.6-44.8\,^\circ\mathrm{C}}{\Longrightarrow} R_I \xrightarrow[45.2\,^\circ\mathrm{C}]{} R_{II} \xrightarrow[46.9\,^\circ\mathrm{C}]{} \text{liquid}.$$

In C25, the sequence of the transition is similar to C23, but there are some differences. In the literature (see the studies [2,18]), the transition $O_i \rightarrow O_{dci}$ in C25 is attributed to a very weak endothermic effect at 38 °C, while on the contrary, in C23 it is related the deviation from the base

line, which precedes the transition into the rotator phase. There is a similar deviation observed in C25, which precedes the peak No. 1 in Figure 2, *c*. In this regard, it can be assumed that the transition $O_i \rightarrow O_{dci}$ occurs at 45.4 °C. But in this case the nature of the effect at 38 °C remains unknown and further research is required, including by synchrotron X-ray diffractometry. Similar to C21 and C23, the peak No. 1 is related to the transition $O_{dci} \rightarrow M_{dci}$ at 47.5 °C, while the peak No. 2 is related to the transition $M_{dci} \rightarrow R_V$ at 48.1 °C, which is confirmed by the literature as well. The continuous transition $R_V \rightarrow R_I$ starts similar to C23 just after the transition into the phase R_V at 48.9 °C. However, according to the literature data, a transition into the phase R_{II} shall be observed around 50 °C. Due to the proximity of the transitions, their peak can merge on the DSC curves, but at 49.9 °C one can note a maximum that is probably related to the DPT into the phase R_{II}. Thus, it may be assumed that the transition $R_V \rightarrow R_I$ ends with a transition into the phase R_{II}. A weak endothermic effect is observed around 52.5 °C, but the literature does not mention phase transitions in this temperature interval. Since it is not possible to determine symmetry of the crystal cell based on the DSC data, then this case also requires X-ray diffraction studies, which are planned by us for C25 in the future. At 53.5 °C, melting starts. Based on the above-given data for C25, the following phase sequence can be determined:

$$O_i \xrightarrow[45.4\,^\circ\mathrm{C}]{} O_{dci} \xrightarrow[47.5\,^\circ\mathrm{C}]{} M_{dci} \xrightarrow[48.1\,^\circ\mathrm{C}]{} R_V \underset{48.9-49.8\,^\circ\mathrm{C}}{\Longrightarrow} R_I \xrightarrow[49.9\,^\circ\mathrm{C}]{} R_{II} \xrightarrow[53.5\,^\circ\mathrm{C}]{} \text{liquid}.$$

By analyzing the DSC thermograms with taking into account the above-described phase sequences, one can note an interrelation of energy of the transition with a transformation type. Thus, the low-energy transitions that are manifested as weak endothermic effects are transitions between the rotator phase, as energy differences of these phases are small. But, on the contrary, a transition the crystal phase–the rotator phase requires a large amount of energy, since the molecules obtain rotational motion, which is manifested on the DSC curves as intense peaks that are the highest of all observed for the solid-solid phase transitions. The transitions between the crystal phases are characterized by an intermediate value of energy and are intensity-average peaks that are different in a dependence on a type of the crystal cells. For example, the transition from one orthorhombic phase into another orthorhombic phase is manifested as a weak deviation from the baseline, since it is a low-energy one, while the transition from the orthorhombic into the monoclinic phase is manifested as a quite intense peak (see the transitions $O_i \rightarrow O_{dci}$ and $O_{dci} \rightarrow M_{dci}$ in Figure 2).

4. Conclusion

As a result of the comprehensive DSC studies done, we were the first to find a sequence of the crystal and rotator phases when heating the odd n-alkanes (heneicosane, tricosane and pentacosane), which turned to be similar for these homologs. The thermograms were analyzed in detail, including in accordance with the diffuse phase transition theory, to reveal a number of new phase transitions. The observed phase transitions were characterized based on literature data for each homolog and with taking into account their maximum similarity in the crystal structure and the chain length. We were the first to find presence of the intermediate orthorhombic phase O_{dci}, the monoclinic phase M_{dci} and the rotator monoclinic phase R_V. And we were the first to reveal the intermediate monoclinic phase M_{dci}. The phase sequence has been proposed for pentacosane according to heneicosane and tricosane. Moreover, we have revealed new thermal effects that require further research.

The results obtained in the study facilitate development of an overall picture of the phase transformations in the long-chain molecular crystals, which are still understudied due to their complexity and many stages.

Conflict of interest

The authors declare that they have no conflict of interest.

References

[1] M.G. Broadhurst. J. Res. Natl. Bur. Stand. **66A**, *3*, 241 (1962).
[2] A.-J. Briard, M. Bouroukba, D. Petitjean, N. Hubert, M. Dirand. J. Chem. Eng. Data **48**, *3*, 497 (2003).
[3] A. Müller. Proc. Royal Soc. Lond. **A127**, 417 (1930).
[4] A. Müller. Proc. Royal Soc. **A138**, *836*, 514 (1932).
[5] E.B. Sirota, H.E. King, D.M. Singer, H.H. Shao. J. Chem. Phys. **98**, *7*, 5809 (1993).
[6] E.B. Sirota, D.M. Singer. J. Chem. Phys. **101**, *12*, 10873 (1994).
[7] S. Nene, E. Karhu, R.L. Flemming, J.L. Hutter. J. Cryst. Growth **311**, 4770 (2009).
[8] E. Blázquez-Blázquez, R. Barranco-García, M.L. Cerrada, J.C. Martínez, E. Pérez. Polymers **12**, *6*, 1341 (2020).
[9] D. Cholakova, K. Tsvetkova, S. Tcholakova, N. Denkov. Colloids Surf. A: Physicochem. Eng. Asp. **634**, 127926 (2022).
[10] C.M. Earnest, J. Jones, A. Dunn. Thermo. **2**, 302 (2022).
[11] J. Doucet, I. Denicolo, A. Craievich. J. Chem. Phys. **75**, *3*, 1523 (1981).
[12] G. Ungar. J. Chem. Phys. **87**, *4*, 689 (1983).
[13] Y. Ogawa, N. Nakamura. Bull. Chem. Soc. Jpn. **72**, 943 (1999).
[14] V.M. Egorov, V.A. Marikhin, L.P. Myasnikova. Polym. Sci. Ser. A **48**, 1270 (2006).
[15] S.A. Gureva, A.K. Borisov, V.A. Marikhin, M.V. Baidakova, E.S. Kulikova, P.V. Dorovatovskii. Phys. Solid State **67**, *4*, 683 (2025). FTT **67**, *4*, 711 (2025). (in Russian).
[16] A.E. Smith. J. Chem. Phys. **21**, 2229 (1953).

[17] L. Robles, D. Mondieig, Y. Haget, M.A. Cuevas-Diarte. J. Chim. Phys. **95**, 92 (1998).
[18] M. Dirand, M. Bouroukba, V. Chevallier, D. Petitjean, E. Behar, V. Ruffier-Meray. J. Chem. Eng. Data **47**, *2*, 115 (2002).
[19] K. Nozaki, N. Higashitani, T. Yamamoto, T. Hara. J. Chem. Phys. **103**, *13*, 5762 (1995).
[20] F. Rajabalee, V. Metivaud, D. Mondieig, Y. Haget, M.A. Cuevas-Diarte. J. Mater. Res. **14**, *6*, 2644 (1999).
[21] B.N. Rolov, V.E. Yurkevitch. Fizika razmytykh fazovykh perekhodov. Izd-vo Rostov. un-ta, Rostov (1983). 350 s. (in Russian).
[22] M. Fisher. The nature of critical points. University of Colorado Press, Boulder, Colorado, U.S.A. (1965). 159 p.
[23] G.A. Malygin. Physics–Uspekhi **44**, 173 (2001).
[24] G.A. Malygin. Phys. Solid State **43**, 1989 (2001).
[25] V.M. Egorov, A.K. Borisov, V.A. Marikhin. Phys. Solid State, **63**, 498 (2021). **63**, *3*, 406 (2021).
[26] G.A. Malygin. FTT **36**, *5*, 1489 (1994). (in Russian).

Translated by M.Shevelev